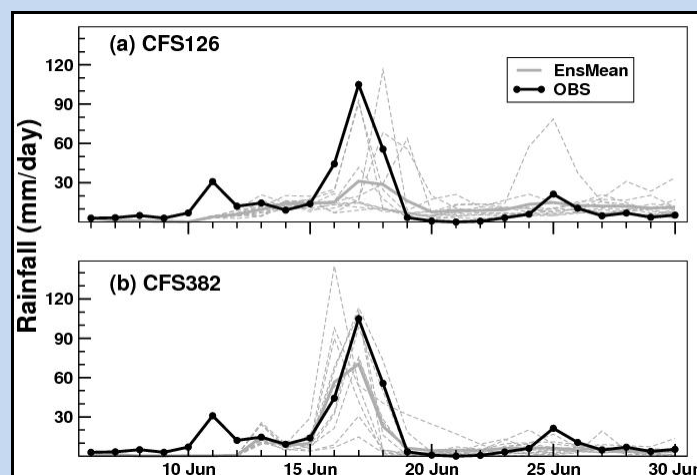


Extended Range Prediction of Uttarakhand Heavy Rainfall Event by an Ensemble Prediction System based on CFSv2



Susmitha Joseph, A.K. Sahai, S. Sharmila, S. Abhilash, N. Borah,
P.A. Pillai, R. Chattopadhyay, Arun Kumar



Indian Institute of Tropical Meteorology (IITM)
Earth System Science Organization (ESSO)
Ministry of Earth Sciences (MoES)
PUNE, INDIA

<http://www.tropmet.res.in/>

Extended Range Prediction of Uttarakhand Heavy Rainfall Event by an Ensemble Prediction System based on CFSv2

Susmitha Joseph¹, A.K. Sahai*¹, S. Sharmila¹, S. Abhilash¹, N. Borah¹, P.A. Pillai¹,
R. Chattopadhyay¹ and Arun Kumar²

¹Indian Institute of Tropical Meteorology, Pune, India

²National Center from Environmental Prediction, Camp Springs, MD, USA

***Corresponding Author Address:**

Dr. A. K. Sahai
Indian Institute of Tropical Meteorology,
Dr. Homi Bhabha Road, Pashan,
Pune – 411 008, INDIA
E-mail: sahai@tropmet.res.in
Ph: +91-20-25904520
Fax: +91-20-25865142



Indian Institute of Tropical Meteorology (IITM)
Earth System Science Organization (ESSO)
Ministry of Earth Sciences (MoES)
PUNE, INDIA
<http://www.tropmet.res.in/>

DOCUMENT CONTROL SHEET

Earth System Science Organization (ESSO)
Ministry of Earth Sciences (MoES)
Indian Institute of Tropical Meteorology (IITM)

ESSO Document Number:

ESSO/IITM/SERP/SR/03(2013)/180

Title of the report:

Extended Range Prediction of Uttarakhand Heavy Rainfall Event by an Ensemble Prediction System based on CFSv2

Author(s) [Last name, First name]

Joseph, Susmitha, Sahai, A.K., Sharmila, S., Abhilash, S., Borah, N., Pillai, P.A., Chattopadhyay, R., Kumar, Arun

Type of Document

Scientific Report (Research Report)

Number of pages and figures

30, 15

Number of references

21

Keywords

Monsoon

Security classification

Open

Distribution

Open

Date of publication

November, 2013

Abstract

This study investigates the scientific rationale behind the fast advancement of 2013 southwest monsoon and the concurrent incidence of a heavy rainfall event in the north Indian state of Uttarakhand. It is found that the interaction between a monsoonal low pressure system and midlatitude systems possibly originated from the Arctic region played seminal role in triggering both events. An ensemble prediction system based on high (T382) as well as low (T126) resolution versions of the coupled general circulation model CFSv2 could predict the extreme event 10-12 days in advance, however they failed to predict the midlatitude influence on the event.

CONTENTS

	Summary	1
1	Introduction	2
2	Methodology	4
	2.1 Model and Observational Datasets	4
3	Results and Discussion	5
	3.1 Local Meteorological Conditions	5
	3.2 Large Scale Features	6
	3.3 Possible role of Arctic Region	7
4	Conclusions and Remarks	8
5	Acknowledgements	9
6	References	10
7	Figures	12

Summary

In 2013, the Southwest monsoon of India covered the entire country one month earlier than its normal date and concurrently, extreme rainfall was experienced in the northern state of Uttarakhand. This study investigates the scientific rationale behind the fast advancement of monsoon and the incidence of the extreme event, with a hypothesis that same meteorological conditions might have triggered both of them. It is found that the interaction between a monsoonal low pressure system and midlatitude systems possibly originated from the Arctic region helped both the early advancement of monsoon and the generation of the heavy rainfall event aided by orographic uplift. The predictability of Uttarakhand event by the ensemble prediction system based on both high (T382) and low (T126) resolution versions of the coupled general circulation model CFSv2 has also been explored. Although the models predicted the event 10-12 days in advance, they failed to predict the midlatitude influence on the event. In both the models, the event was produced by the generation and northwestward movement of low pressure system developed in Bay of Bengal.

1. Introduction

Southwest (SW) monsoon of 2013 has been very unique in terms of its timely onset, and rapid advancement (**Figure 1**). The season, particularly the first two months, June and July, witnessed unprecedented amount of rainfall which was about 120% of its long period average. Several parts of North India, Northeast India and Southern Peninsula experienced floods during this monsoon season. The first in the series was the devastating Uttarakhand flash floods, which affected the lives of thousands of people. Though heavy rainfall was experienced over parts of Himachal Pradesh, Haryana, Delhi and Uttar Pradesh in India in addition to some regions of Western Nepal and Western Tibet, more than 95% of casualties occurred in Uttarakhand alone (source: http://en.wikipedia.org/wiki/2013_North_India_floods).

The Indian state of Uttarakhand and adjoining areas received unparalleled rainfall from 14-17 June 2013. A landslide caused by the heavy rainfall might have blocked the Mandakini River and the water that was dammed behind the landslide might have gushed out in the early morning of 17 June (Srinivasan, 2013). Landslides, due to the floods, damaged several houses and structures, killing those who were trapped. The roads were seriously damaged at several places, resulting in huge traffic jams, and the floods caused valuable properties including vehicles to be washed away. Thousands of pilgrims to the pilgrimage centers in the region were stranded for more than three days with little or limited food. According to environmentalists, unscientific developmental activities undertaken over the region in the recent decades contributed to the high level loss of property and lives (source: http://en.wikipedia.org/wiki/2013_North_India_floods).

A similar extreme rainfall event happened in late July–early August of 2010 in Pakistan. During that time, a long-lived blocking high was present over Europe and Russia. The interaction between the tropical monsoon surges and the extratropical disturbances downstream of the European blocking was responsible for the severe flooding in Pakistan (Hong et al., 2011; Wang et al. 2011; Lau and Kim, 2012). Hong et al. (2011) advocated that the southward penetration of the cold-dry high potential vorticity (PV) air associated with the trough east of the blocking induced anomalous low-level convergence and upward motion and provided a favorable environment for the northward propagation of monsoon surges over the region. Houze et al. (2011) noted that the rain storms that caused the Pakistan flood were associated with the anomalous propagation of a depression formed in BoB. The development

of high pressure over Tibetan Plateau also favored the occurrence of a synoptic-scale channel of anomalously moist flow toward the mountain barrier and created an environment in which the precipitating mesoscale cloud systems (MCSs) took on a form that included broad stratiform rain regions lying over the slopes of the Himalayas. The areal coverage of these wide raining systems contributed to the huge runoff and flooding event (Houze et al., 2011). According to Wang et al. (2011), the MCSs occurred during the period when a series of midlatitude troughs intruded south. Hence, it may be noted that the tropical-extratropical interaction can cause extreme rainfall events in the orographic regions.

In 2013, monsoon arrived Kerala coast on 01 June (its climatological date) and covered the entire country by 16 June, almost one month ahead of its normal date, 15 July (**Figure 1**). After setting over Kerala, the SW monsoon rapidly progressed northward (see **Figure 2**). The monsoon current was exceptionally strong and an offshore trough over the west coast became very strong from 07 June onwards. By 11 June, the monsoon covered up to Gujarat and for the next two days, a cyclonic circulation was noticed over the region. On 12 June, a cyclonic circulation developed in Bay of Bengal (BoB) region and moved northwestward to the Indian land. The cyclonic circulation was anomalously strong over the north and northwest India from 15 June onwards. The active offshore trough together with the low pressure system might have pulled the monsoon current northward and helped the monsoon to cover the entire country by 16 June.

As seen from **Figure 1**, monsoon covered the entire country by 16 June and the Uttarakhand event happened on 16-17 June. As both events occurred concurrently, it is possible that both were linked to each other and might be governed by same meteorological conditions. In this study, we attempt to unravel the scientific reason behind the rapid advancement of monsoon and occurrence of the extreme rainfall event. Many people speculated that the heavy rainfall occurred over Uttarakhand was due to cloudburst, a local phenomenon that causes rainfall with intensity above 100 mm/hr. Srinivasan (2013) indicated that the Uttarakhand event was triggered by the interaction between a midlatitude weather system and the monsoon. Hence in this study, we investigate whether the extreme event was triggered by local or large scale features. Furthermore, whether the same meteorological conditions helped monsoon to cover the entire country one month earlier? Webster et al. (2011) demonstrated that Pakistan flood, which was forced by midlatitude systems, was predictable by 6-8 days in advance. Therefore, in this study, we pose the following question

as well: If the Uttarakhand event was forced by large scale conditions and, whether it could be predicted a few days in advance?

The prediction of Uttarakhand event on extended range time scale has been assessed by an Ensemble Prediction System (EPS) indigenously developed by the extended range prediction (ERP) group of Indian Institute of Tropical Meteorology (IITM), Pune, India. The ERP group at IITM has been providing the extended range prediction of active/break spells of Indian summer monsoon since 2011 up to 4 pentad lead using the EPS based on the ocean-atmosphere coupled Climate Forecast System version 2 (CFSv2) model (Abhilash et al., 2012, 2013; Borah et al., 2013). The EPS produces 11 member ensemble forecasts for 45 days lead time at every 5 day, starting from 16 May to 28 September of every year. The forecasts for 2013 monsoon season is available at the IITM website <http://www.tropmet.res.in/erpas/> and the forecasts were being updated every 5 day.

2. Methodology

2.1 Model and observational datasets

The coupled model used in the study is the latest version of National Centers for Environmental Prediction (NCEP) CFSv2 [Saha et al., 2013; submitted manuscript] which is run at a horizontal resolution of T126 (~100km; hereafter termed as CFS126) and T382 (~38 km; hereafter termed as CFS382) with 64 vertical levels. The atmospheric component of the model is the NCEP Global Forecast System (GFSv2) which is coupled to the GFDL Modular Ocean Model version 4p0d [MOM4; Griffies et al., 2004], sea-ice model and land surface model. Details of the model and the formulation of EPS can be found in Abhilash et al. (2012, 2013) and Borah et al. (2013).

For the observations, the IMD-TRMM merged rainfall dataset (Mitra et al., 2009) and the National Center for Environmental Prediction/National Center for Atmospheric Research (NCEP/NCAR) Reanalysis datasets (Kalnay et al., 1996) have been used. The meteorological parameters utilized from NCEP/NCAR reanalysis for the study are: zonal, meridional and vertical components of wind, specific humidity, air temperature and geopotential height at pressure levels and also mean sea level pressure (mslp). Additionally, we have computed the potential vorticity (PV), moisture convergence, stream function and rotational winds.

3. Results and Discussion

The ability of the EPS in predicting Uttarakhand rainfall event 10-20 days in advance (from 26 May (0526), 31 May (0531) and 05 June (0605) initial conditions) has been examined (Figure not shown) and it is found that the event was predicted well from 0605 initial condition (**Figure 3**). Therefore, results from 0605 initial condition will be discussed and compared with observations hereafter. The northward propagation of rainfall (averaged over Indian longitudes 70°-90°E) predicted from 0605 initial condition by CFS126 and CFS382 are plotted and compared with observations in **Figure 4**. It is clear from the figure that both CFS126 and CFS382 could predict the evolution of rainfall realistically.

3.1 Local meteorological conditions

As mentioned earlier, the offshore trough was active over the west coast from 07 June onwards and a low pressure system developed on 12 June in BoB. The development of low pressure system over BoB and its northwestward movement to the Indian land has been predicted very well by CFS126 and CFS382 (**Figure 5 to 7**). **Figure 5** depicts the rainfall and 850 hPa circulation predicted by CFS126 and CFS382 5-10 days in advance. The rainfall over the west coast is overestimated in both CFS126 and CFS382. The cyclonic circulation associated with the low pressure system are predicted reasonably well by both versions of CFS, however, the magnitude of rainfall over Uttarakhand region (78°-80°E; 29°-31°N) is much more realistic in CFS382 than CFS126 (refer **Figure 3** and **5**). **Figure 6** and **7** portrays the moisture convergence anomaly (vertically integrated up to 500 hPa; shaded) together with mslp (contour) and PV anomaly (shaded)_at 700 hPa respectively, for observations as well as CFS126 and CFS382. The northwestward movement of moisture convergence anomaly (**Figure 6A**) and PV anomaly (**Figure 7A**) is associated with the low pressure system (evident from the mslp contours) that developed over BoB, which then moved towards northwest India and dissipated near the foothills of Himalayas over Uttarakhand region. Both versions of CFS could predict these features reasonably well, with CFS382 performing slightly better (**Figure 6B-C** and **Figure 7B-C**). However the moisture convergence anomalies are stronger in both of them.

3.2 Large scale features

The Pakistan flood of 2010 resulted from the interaction between tropical and extratropical weather systems (Hong et al. 2011, Wang et al. 2011). In order to get an insight into the role of large scale extratropical features on the occurrence of Uttarakhand event, the spatial distribution of large scale dynamical parameters over a larger region are examined in this section. **Figure 8A-C** shows the evolution of tropospheric temperature (TT; air temperature averaged between 600-200 hPa; Xavier et al. 2007) anomalies and geopotential height anomalies at 500 hPa, for observations, CFS126 and CFS382 respectively. It is interesting to note that cold-dry air from Arctic region descend down the latitudes to the Indian region with time (**Figure 8A**). By 16 June, the cold air anomaly got separated from its polar branch and got sandwiched between warm temperature anomalies. This has caused an atmospheric blocking of the cold-dry air, which in turn might have destabilized the atmosphere over the Uttarakhand region during 16-17 June. The colder temperature anomalies are collocated with the negative geopotential height anomalies. This clearly illustrates the seminal role of midlatitude systems in triggering the extreme rainfall event. **Figure 9** displays circulation at 200 hPa level, with its magnitude shaded. During 12 and 13 June, the tropical easterly jet (TEJ) is very strong (**Figure 9A**). From 14 June onwards, the intrusion of westerly winds to the South Asian region is noticed. On 15-16 June, the westerlies are stronger and they penetrate to the Indian land. Similar signals are noted in **Figure 10**, which displays the anomalies of stream function and rotational wind at 200 hPa. The stream function anomalies (**Figure 10A**) are consistent with that of TT (**Figure 8A**), illustrating the incursion of systems from Arctic region to the Indian region. However, these features are totally absent in the CFS126 (**Figure 8B, 9B and 10B**). Although midlatitude intrusion is noted in stream function and circulation anomalies in CFS382, it is not from the right direction (**Figure 9C and 10C**).

The extratropical influence on the extreme event can be clearly seen in the time-height plot of temperature and zonal wind anomalies, averaged over Uttarakhand region (**Figure 11**). The incursion of cold temperature anomalies from upper levels to the lower levels is noticed around 15 June, which then persisted up to around 20 June (**Figure 11A**). It is interesting to note that easterly wind anomalies descend down to the region around 17 June. The zonal wind anomalies are baroclinic in nature from 15-17 June. This might have helped the system to intensify and give torrential rainfall over the region. The penetration of

cold temperature anomalies is missing in CFS126 as well as CFS382 (**Figure 11B and C**). It is also noticed that the colder temperature anomalies in the lower levels noted after 13 June in CFS126 and CFS382 prevails over the region till June end. This feature was not observed in reality. However, the intrusion of easterly anomalies is noted in both CFS versions. **Figure 12** presents the time-height evolution of the anomalies of PV and vertical velocity (pressure vertical velocity multiplied by -1.0) over Uttarakhand region. In observations, the strong positive PV anomalies penetrate from upper levels to the lower levels and intense ascending motion (extending even up to 200 hPa, probably aided by orographic lifting) is observed at lower levels on 17 June (**Figure 12A**). Nevertheless, the penetration of positive PV anomalies are absent in CFS126. Although ascending motion is obvious in CFS126, it is not as strong as in observations. In CFS382, the ascending motion is stronger than observations. The preponderance of extratropical systems on the Uttarakhand event is evident in the Hovmüller diagram of the anomalies of PV at 315K and vertically integrated (surface to 500 hPa) specific humidity (**Figure 13**). The anomalies are averaged over longitudes of Uttarakhand during 16-17 June. It is noticed from the figure that strong positive PV anomalies penetrated from extratropics southward to the Indian region. Concurrently, strong positive PV anomalies corresponding to the low pressure system developed over BoB were moving northward to reach the Uttarakhand region (**Figure 13A**). This coincides well with the high moisture content over the region. It is to be perceived from **Figure 13B-C** that the southward penetration of positive PV anomalies from extratropical region is totally absent in CFS126 as well as CFS382.

3.3 Possible role of Arctic Region

The above results reveal that formation of low pressure system in BoB around 12 June and the southward advection of cold dry extratropical air, and their interaction might have played influential role in the rapid advancement of monsoon and the incidence of Uttarakhand rainfall event. Still there remains an open question – what triggered the midlatitude disturbances that affected the Indian region? It was noted in **Figure 8 and 10** that the disturbances were originated from the Arctic region. The dominant variability in the Arctic region is the Arctic Oscillation (AO; Lorenz, 1950; Thompson and Wallace, 1998), described in terms of the AO index, defined by the variations in the surface atmospheric pressure patterns north of 20° N latitude. The AO index is constructed by projecting the daily mean 1000-hPa height anomalies onto the leading EOF mode of 1000-hPa height anomalies

poleward of 20° latitude for the Northern Hemisphere. When AO index is positive, surface pressure is low in the polar region. This helps the middle latitude jet stream to blow strongly and consistently from west to east, thus keeping cold Arctic air locked in the polar region. When the AO index is negative, there tends to be high pressure in the polar region, weaker zonal winds, and greater movement of frigid polar air into middle latitudes. Although AO is weak in the spring season, it is still the leading mode in the inactive seasons (Thompson and Wallace, 2000). Studies reveal that the spring time AO can have significant influence on the Asian summer monsoon circulation and rainfall (Gong and Ho, 2003). It is worthwhile to note that AO was in its negative phase in the spring season of this year (**Figure 14**), which might have caused the polar cold dry air to meddle with the tropical atmosphere. Another possibility that caused the intrusion of Arctic air to the tropics could be related to the recent Arctic warming. During the past few decades, the Arctic has warmed almost twice as large as the global average (Screen and Simmonds, 2010). Enhanced warming over the Arctic region can slacken the jet streams and produce larger north-south meanders in the flow. These meanders can cause the mid-latitude weather systems to be more persistent and increase the probability of extreme weather events by developing blocking patterns (Francis and Vavrus, 2012). It is known that cold air intrusions can trigger wet spells in a humid atmosphere (Li and Fu, 2006). So, it could be speculated that the midlatitude disturbances generated from the Arctic region intruded to the Indian region and interacted with the low pressure system in BoB associated with the monsoon current. This interaction might have helped the monsoon to cover the entire country by 16 June and caused excessive rainfall in the orographic region.

Though CFS126 and CFS382 predicted the extreme rainfall event 10-12 days in advance, the midlatitude influence has entirely gone astray. In both CFS126 and CFS382, the low pressure system that developed in BoB on 12 June was predicted well in advance and it is the same system aided by orographic lifting gave enormous rainfall in the mountainous Uttarakhand region and helped monsoon to cover the entire country by 16 June.

4 Conclusions and Remarks

This study examines the rationale behind the rapid advance of SW monsoon 2013 and the concurrent occurrence of the extreme rainfall event in Uttarakhand. It is found that during 14-17 June 2013, tropospheric cold temperature anomalies emanated from the Arctic region penetrated down the latitudes and moved towards the Indian region. These cold temperature anomalies got blocked between warm temperature anomalies and intruded from upper levels

to lower levels over Uttarakhand region around 17 June. This might have destabilized the atmosphere over the region. Simultaneously, a low pressure system that developed over BoB on 12 June moved inland, supplied moist air to the region and interacted with the midlatitude systems. The cold air intrusion in the presence of humid atmosphere along with orographic uplift might have triggered excessive amount of rainfall over the region.

The strength of an EPS based on higher and lower resolutions of CFSv2 (CFS382 and CFS126 respectively) in predicting the heavy rainfall event has also been examined. It is noticed that both CFS126 and CFS382 could predict the extreme event 10-12 day in advance, with CFS382 performing better in predicting the magnitude of rainfall. Even the formation and northwestward movement of the low pressure system over BoB is better predicted by CFS382. However, both the models failed to predict the extratropical influence on the event. It is revealed that the anomalous moist flow of monsoonal surges (which are associated with the low pressure system) to the mountainous region (as noted by Houze et al., 2011 in the case of Pakistan flood event) generated the extreme event in the models, especially in CFS382 (evident from the stronger ascending motion over the region). Hence, it may be concluded that higher resolution models could be useful in the ERP of extreme events and the formation of cyclonic systems. However, they need to be improved in order to predict the teleconnection patterns realistically.

5. Acknowledgements

IITM is fully supported by Ministry of Earth Sciences, Govt. of India. We are thankful to Prof. B.N. Goswami, Director, IITM for his encouragement and support. SS is grateful to CSIR for financial assistance. We are thankful to Dr. J.R. Kulkarni for the constructive comments and suggestions on the manuscript. We also thank Dr. D.R. Sikka and Dr. M. Rajeevan for useful discussions. The model runs are carried out on Prithvi IBM High Performance Computing System installed at IITM, Pune.

6. References

- Abhilash, S., Joseph S., Chattopadhyay R., Pattnaik S., Krishna P.M., De S., Sahai A.K. and Goswami B.N., 2012, Performance of an Ensemble Prediction System based on CFSV2 for the Extended Range Prediction of Active-Break Spells of Indian Summer Monsoon Rainfall during 2011, IITM Research Report, No. RR-128.
- Abhilash, S., Sahai A.K., Pattnaik S., Goswami B.N. and Kumar A., 2013, Extended Range Prediction of Active-Break Spells of Indian Summer Monsoon Rainfall using an Ensemble Prediction System in NCEP Climate Forecast System. *Int. J. Climatol.*, DOI: 10.1002/joc.3668
- Borah, N., Abhilash, S., Joseph, S., Chattopadhyay, R., Sharmila, S., and Sahai, A.K., 2013, Development of Extended range prediction system using CFSv2 and its verification, IITM Research Report, RR-130.
- Francis, J.A., and Vavrus. S.J., 2012, Evidence linking Arctic amplification to extreme weather in mid-latitudes, *Geophys. Res. Lett.*, 39, L06801, doi:10.1029/2012GL051000
- Gong, D.-Y., and Ho, C. -H., 2003, Arctic Oscillation signals in the East Asian summer monsoon, *J. Geophys. Res.*, 108, doi:10.1029/2002JD002193
- Griffies, Stephen M., Matthew J. Harrison, Ronald C. Pacanowski and Anthony Rosati, 2004, A Technical Guide to MOM4, GFDL Ocean Group Technical Report No. 5, Princeton, NJ, NOAA/Geophysical Fluid Dynamics Laboratory, 342 pp
- Hong, C.-C., Hsu, H.-H., Lin, N.-H., Chiu, H., 2011, Roles of European Blocking and the tropical-extratropical interaction in the 2010 Pakistan flooding, *Geophys. Res. Lett.*, 38, L13806, doi:10.1029/2011GL047583
- Houze, R. A., Rasmussen, K. L., Medina, S., Brodzik, S. R., and Romatschke, U., 2011, Anomalous atmospheric events leading to the summer 2010 floods in Pakistan, *Bull. Amer. Met. Soc.*, doi:10.1175/2010BAMS3173.1
- Kalnay, E. et al., 1996, The NCEP/NCAR 40-year reanalysis project, *Bull. Amer. Met.Soc.*, 77, doi:10.1175/1520-0477
- Lau, W.K.M. and Kim, K.-M., 2012, The 2010 Pakistan flood and Russian heat wave: teleconnection of hydrometeorological extremes, *J. Hydromet.*, 13, pp 392-403, DOI: 10.1175/JHM-D-11-016.1

- Li, W. and Fu, R., 2006, Influence of cold air intrusions on the wet season onset over Amazonia, *J. Clim.*, 19, pp 257-275
- Lorenz, E.N., 1950, Seasonal and irregular variations of the Northern Hemisphere sea level pressure profile, *J. Meteor.*, 8, 52-59.
- Mitra, A.K., Bohra A.K., Rajeevan, M. and Krishnamurti, T.N., 2009, Daily Indian precipitation analyses formed from a merged of rain-gauge with TRMM TMPA satellite derived rainfall estimates, *Journal of Meteorological Society of Japan*, 87A, 265-279.
- Saha, S. and *et. al.*, 2013, The NCEP Climate Forecast System Version 2. Submitted, *J. Clim.*, http://cfs.ncep.noaa.gov/cfsv2.info/CFSv2_paper.pdf
- Screen, J.A., and Simmonds, I., 2010, The central role of diminishing sea ice in recent Arctic temperature amplification, 464, doi:10.1038/nature09051
- Srinivasan, J., 2013, Predicting and managing extreme rainfall, *Curr. Sci.*, 105, No.1, 10 July 2013
- Thompson, D.W.J. and Wallace, J.M., 1998, The Arctic oscillation signature in the wintertime geopotential height and temperature fields, *Geophys. Res. Lett.*, 25, 1297-1300
- Thompson, D.W. J. and Wallace, J.M., 2000, Annular modes in the extratropical circulation, Part-I, Month-to-month variability, *J. Clim.*, 13, 1000-1016
- Wang, S.-Y., Davies, R.E., Huang, W.-R. and Gillies R. R., 2011, Pakistan's two-stage monsoon and links with the recent climate change, *J. Geophys. Res.*, 116, D16114, doi:10.1029/2011JD015760
- Webster, P.J., Toma V.E. and Kim, H.-M., 2011, Were the 2010 Pakistan floods predictable?, *Geophys. Res. Lett.*, 38, L04806, doi:10.1029/2010GL046346
- Xavier, P. K., Marzin, C., and Goswami, B. N., 2007, An objective definition of the Indian summer monsoon season and a new perspective on ENSO-monsoon relationship, *Q. J. Meteorol. Soc.* 133, 749-764

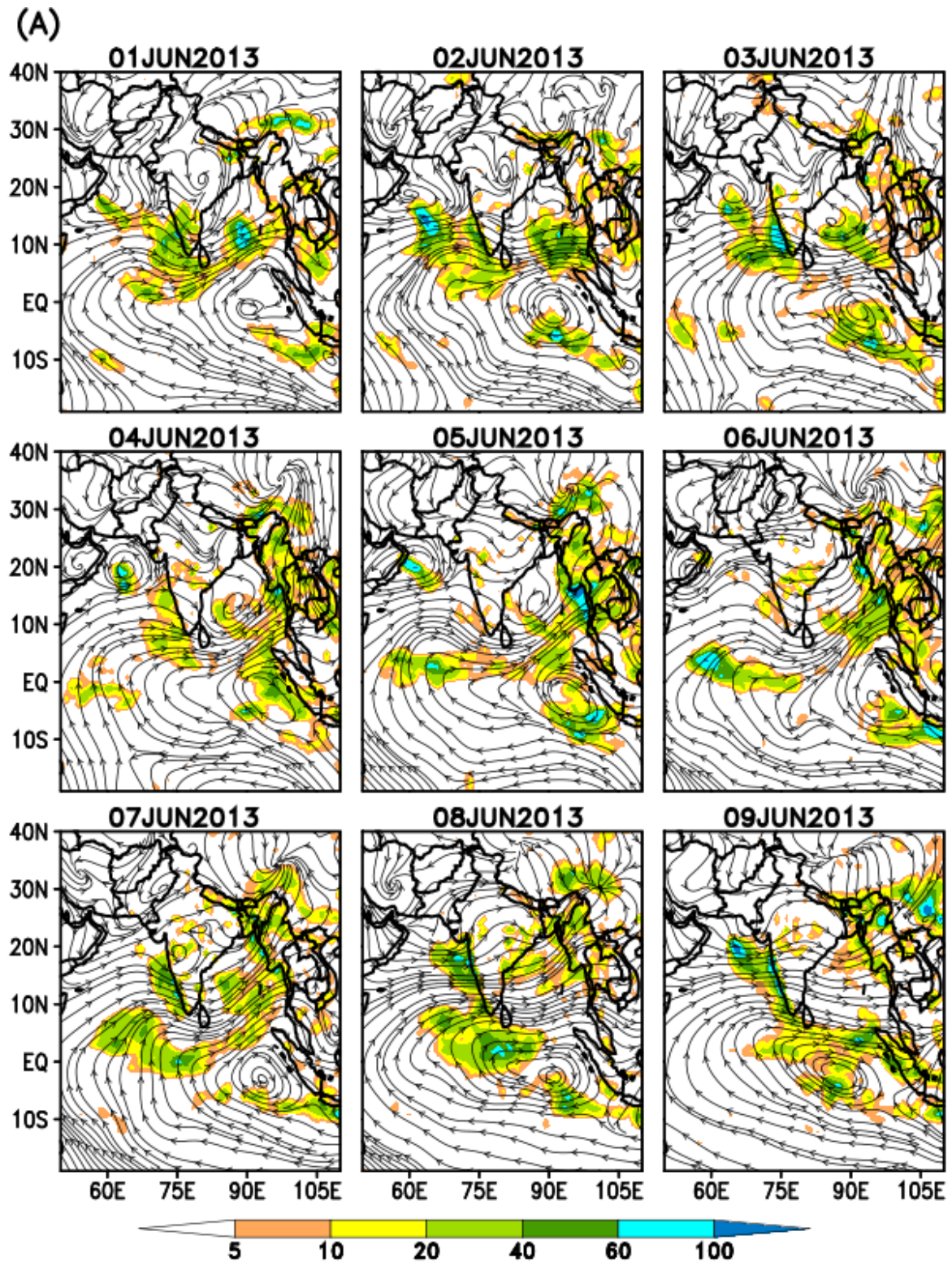


Figure 2: Progression of actual rainfall (mm day^{-1} ; *shaded*) and 850 hPa wind (ms^{-1} ; *streamline*) during SW monsoon 2013 from observations.

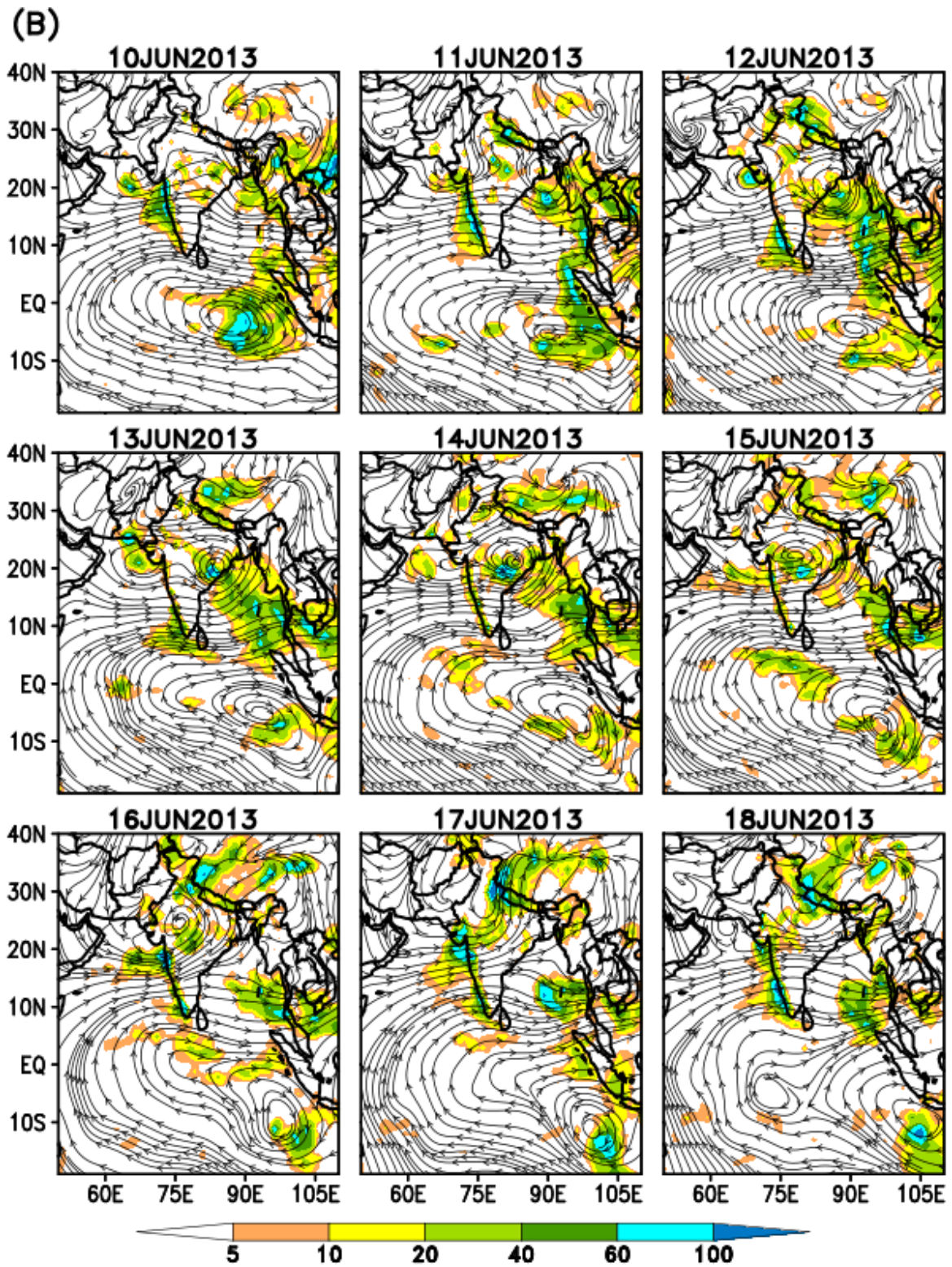


Figure 2: (contd...)

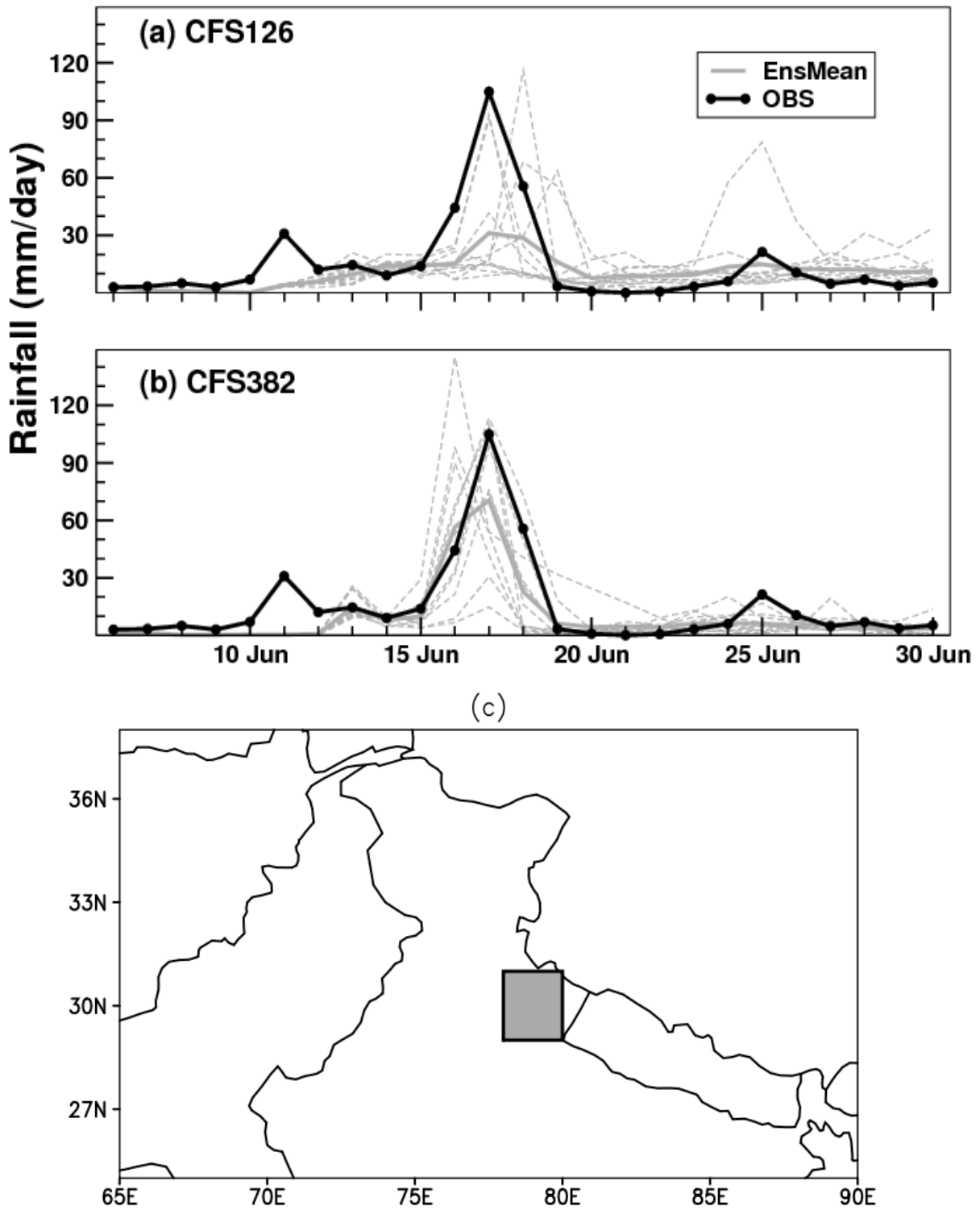


Figure 3: Extended range prediction of Uttarakhand rainfall event by (a) CFS126 and (b) CFS382 from 05 June initial condition. The region where rainfall values are averaged is shown in (c)

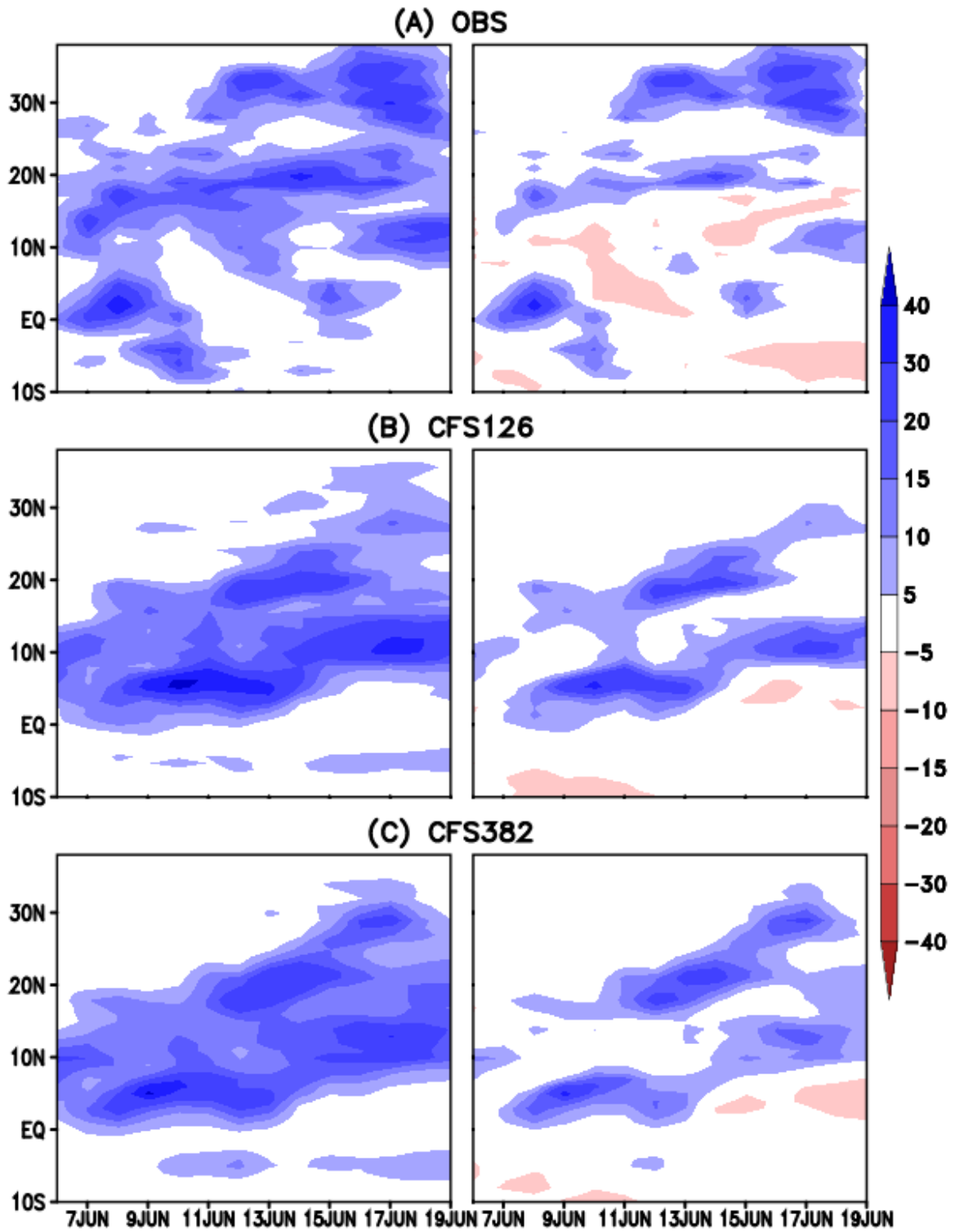


Figure 4: Propagation characteristics of actual rainfall (*left panel*) and rainfall anomalies (*right panel*) for (A) OBS, (B) CFS126 and (C) CFS382. Unit: mm day^{-1}

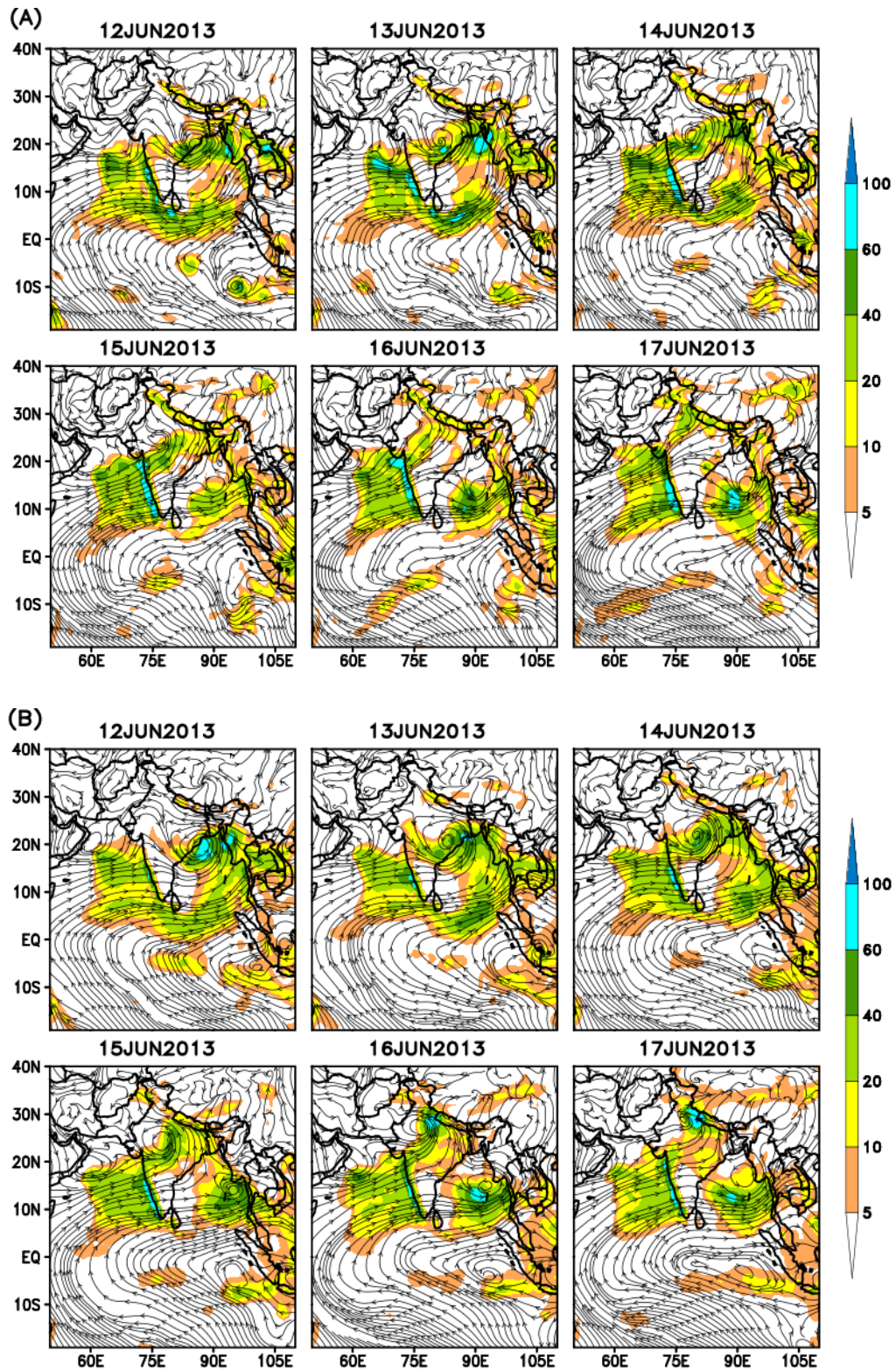


Figure 5: Evolution of rainfall (mm day^{-1} ; *shaded*) and 850 hPa circulation (ms^{-1} ; *streamline*) as predicted by (A) CFS126 and (B) CFS382

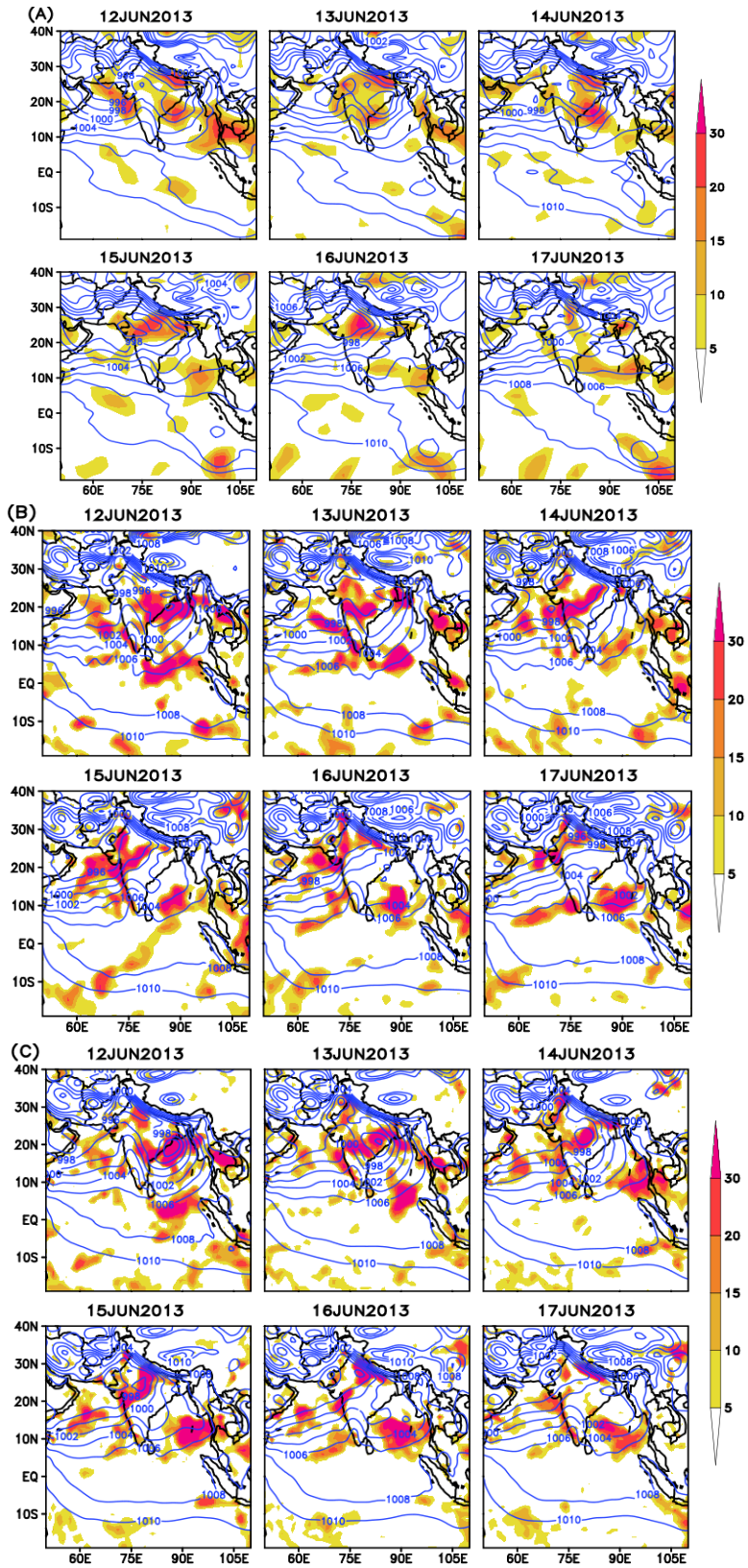


Figure 6: Evolution of anomalies of vertically integrated (surface to 500 hPa) moisture convergence (mm day^{-1} ; shaded) and mean sea level pressure (hPa; contour) in (A) OBS (B) CFS126 and (C) CFS382

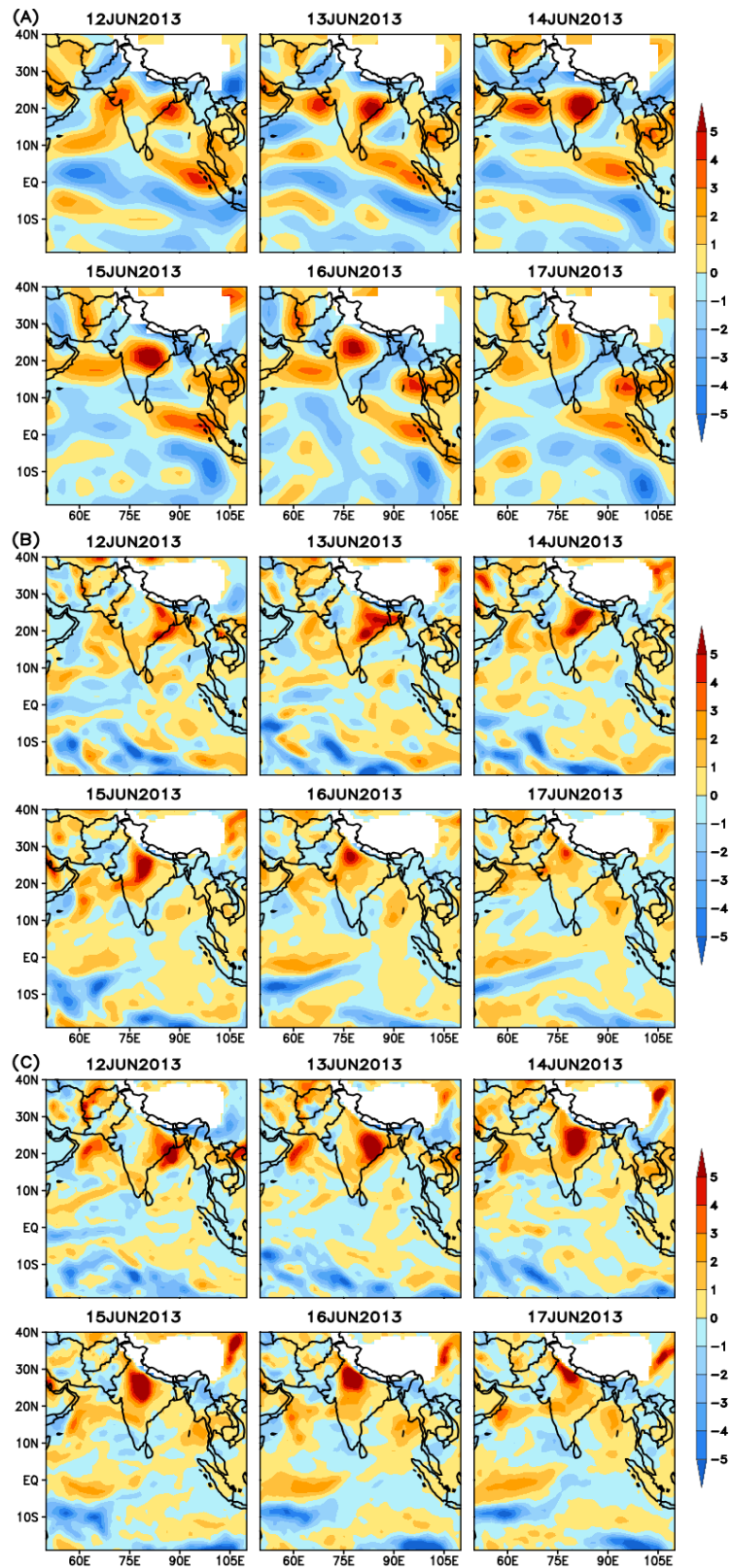


Figure 7: Same as Figure 6, but for anomalous Potential Vorticity (PV; $\times 10^{-7} \text{ s}^{-1}$) at 700 hPa

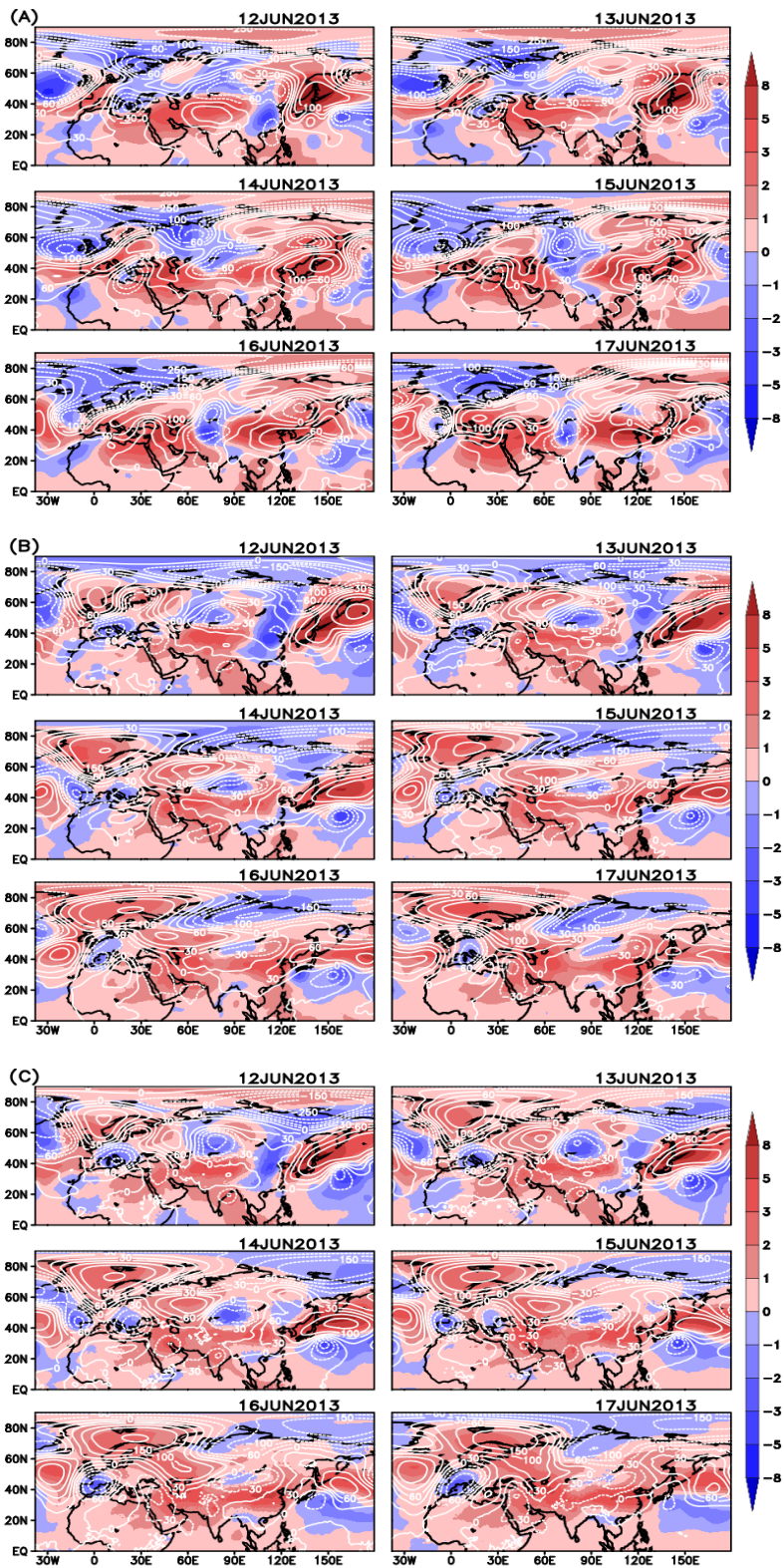


Figure 8: Same as figure 7, but for anomalies of tropospheric temperature (TT; Kday^{-1} ; shaded) and 500 hPa geopotential height (m; contour)

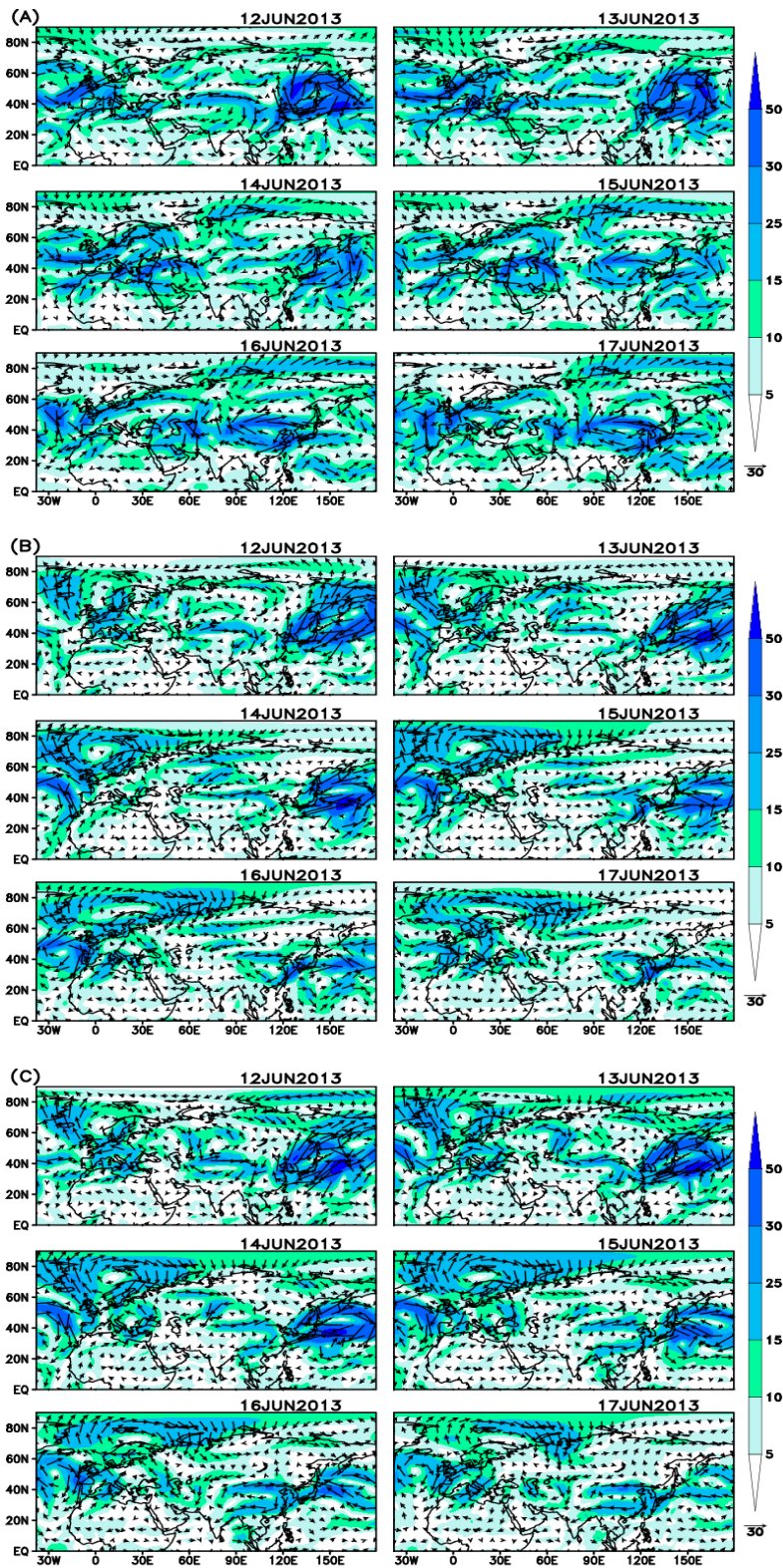


Figure 9: Same as figure 7, but for 200 hPa wind (ms^{-1}) anomalies. The magnitude of wind is shaded.

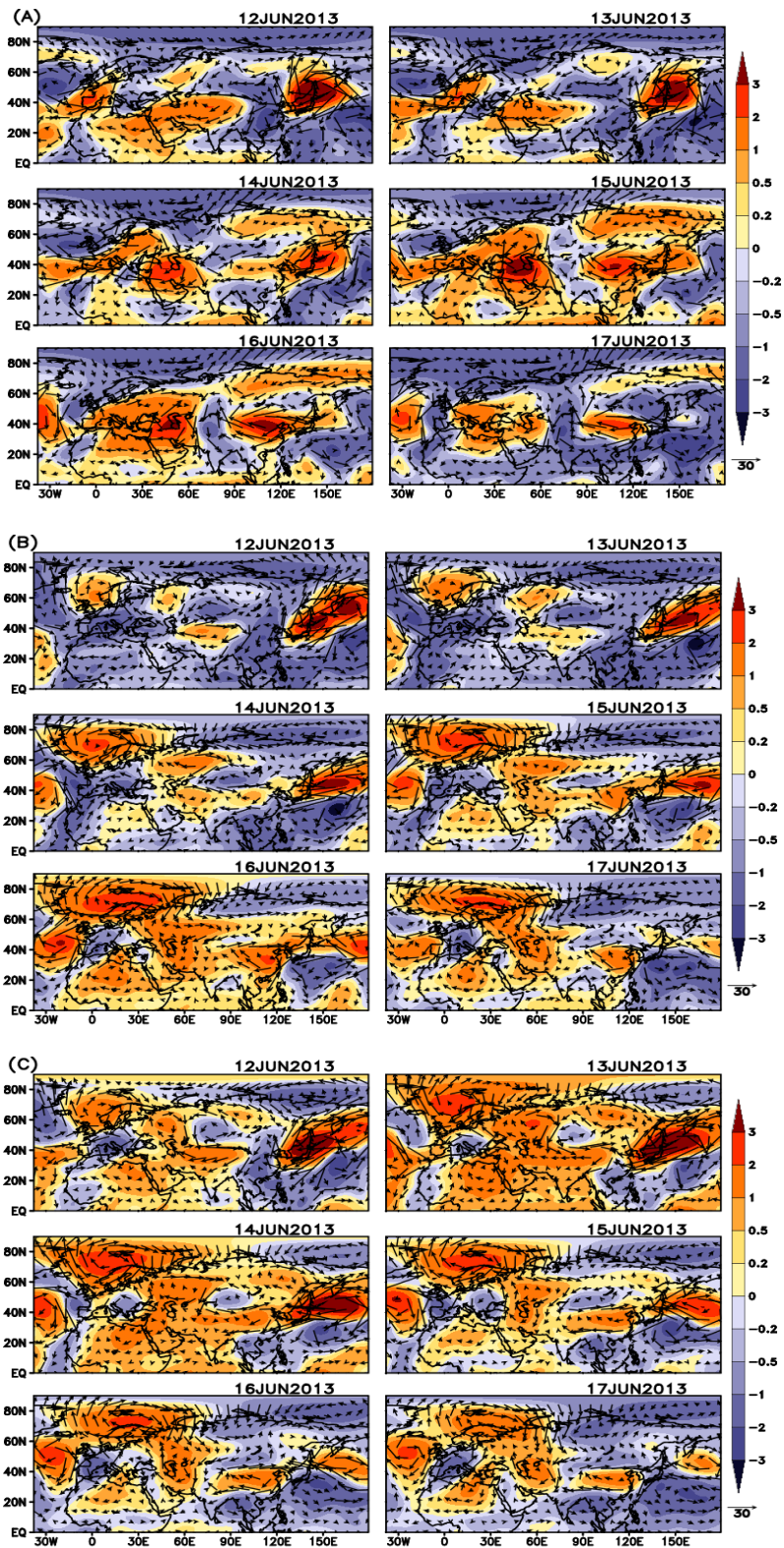


Figure 10: Same as figure 7, but for stream function ($\times 10^{-7} \text{ m}^2 \text{ s}^{-1}$; *shaded*) and rotational wind (ms^{-1} ; *vector*) anomalies at 200hPa

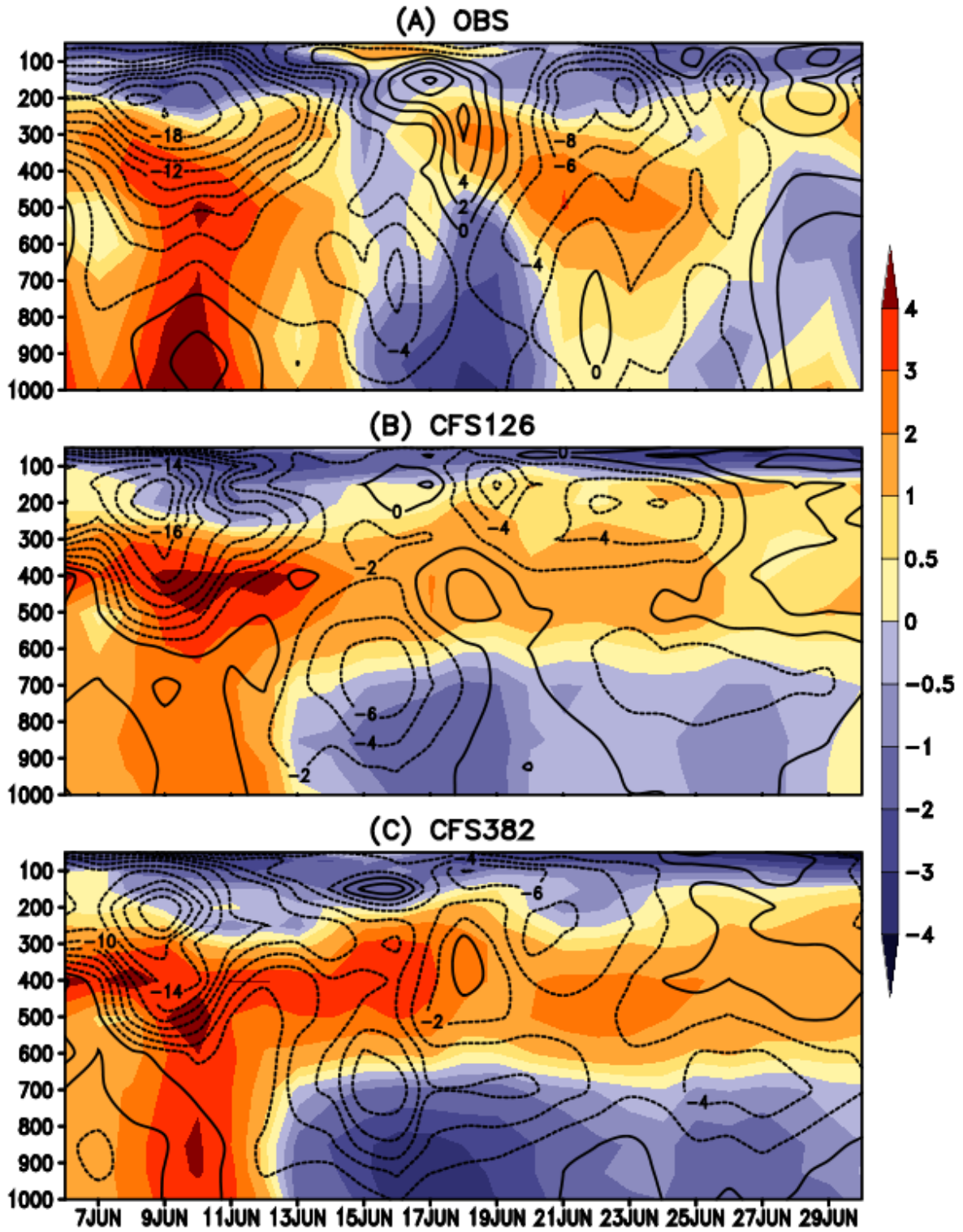


Figure 11: Time-height evolution of temperature (K day^{-1} ; *shaded*) and zonal wind (m s^{-1} ; *contour*) anomalies over Uttarakhand region (averaged over $78\text{-}80^{\circ}\text{E}$; $29\text{-}31^{\circ}\text{N}$)

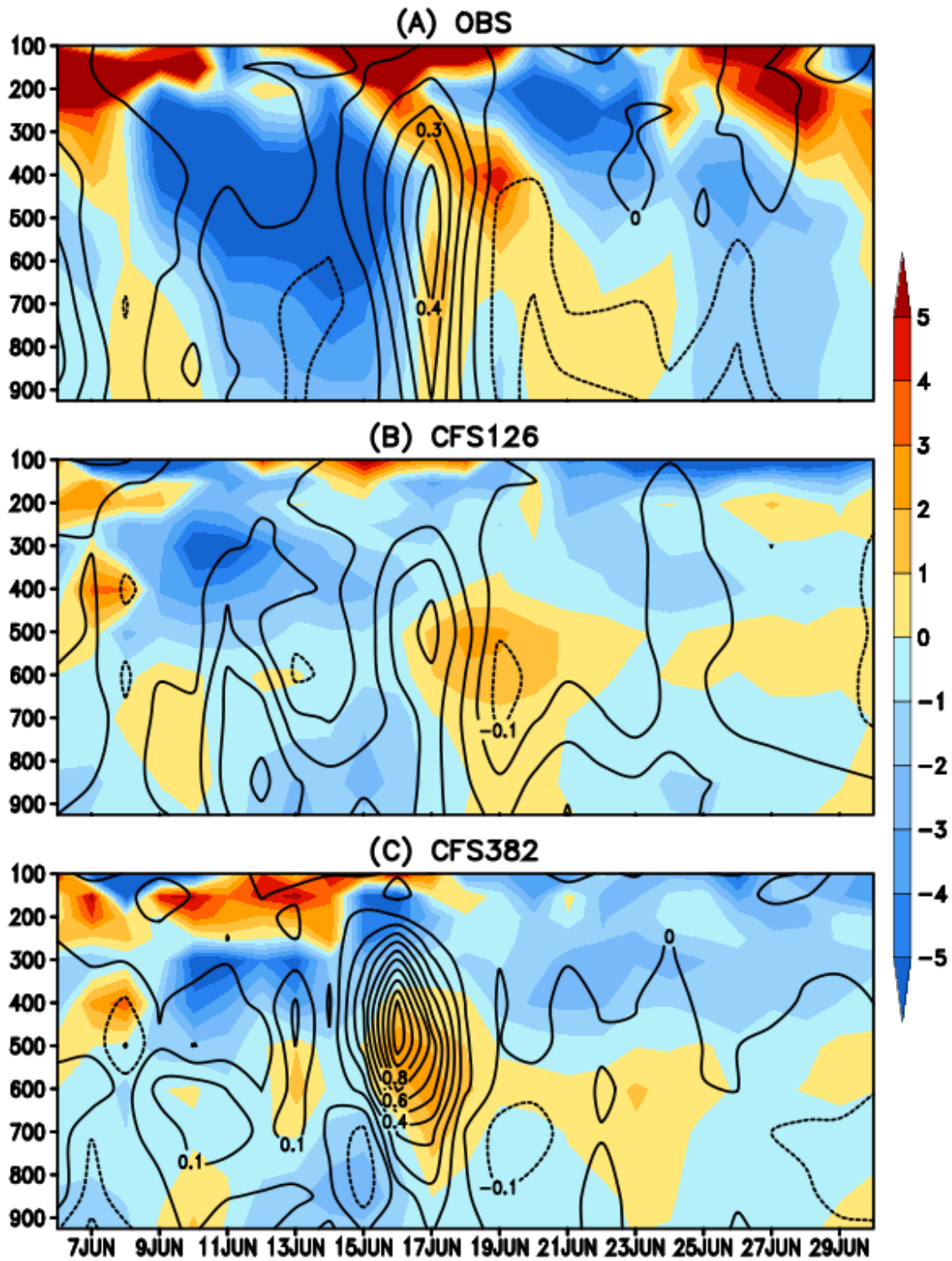


Figure 12: Same as figure 11, but for anomalies of Potential Vorticity (PV; $\times 10^{-7} \text{ s}^{-1}$; *shaded*) and omega (pressure vertical velocity multiplied by -1.0; hPa s^{-1} ; *contour*)

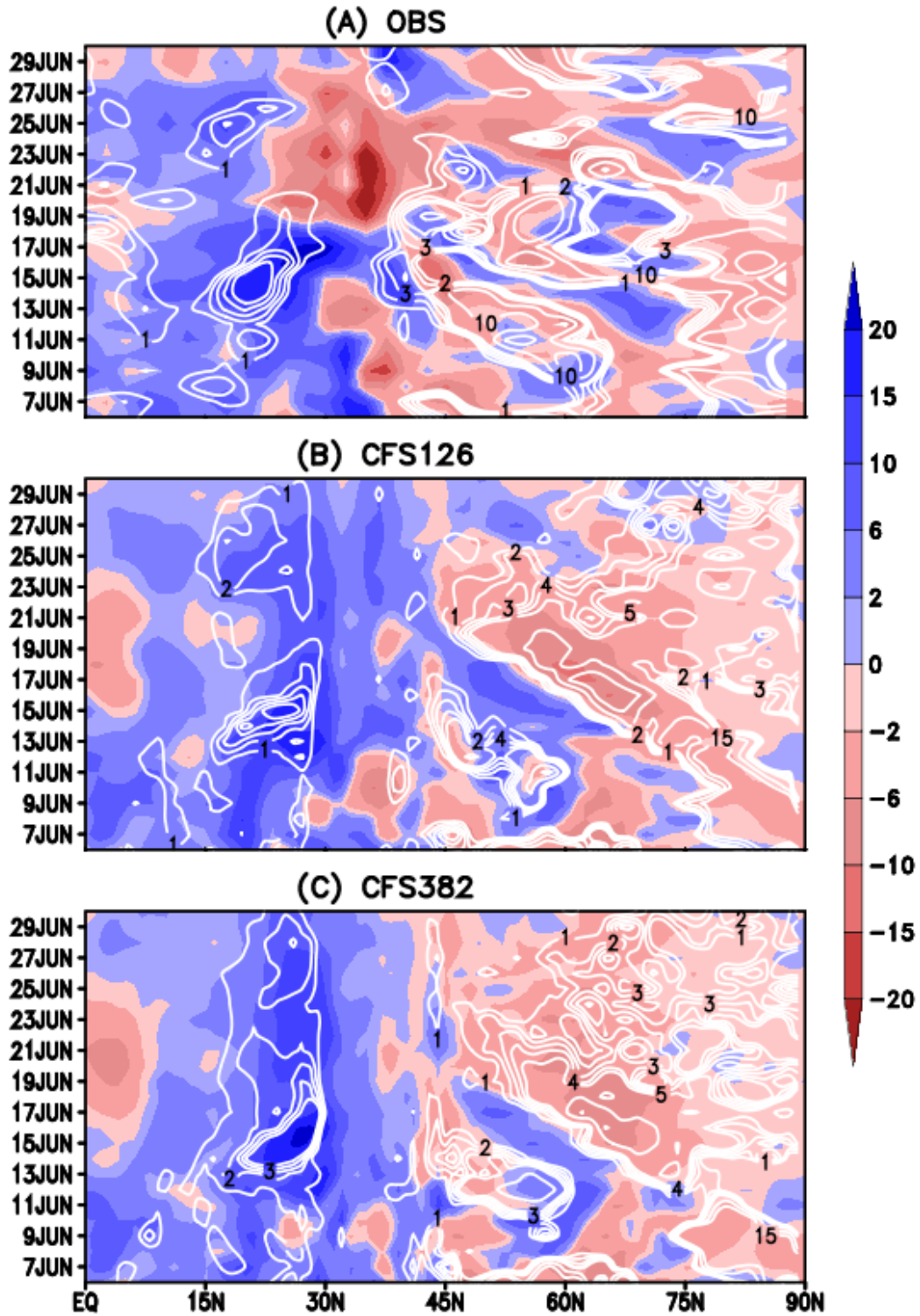


Figure 13: Time-latitude evolution of the anomalies of vertically integrated (from surface to 500 hPa) specific humidity (mm day^{-1} ; *shaded*) and potential vorticity at 315K ($\times 10^{-7} \text{ s}^{-1}$; *contour*)

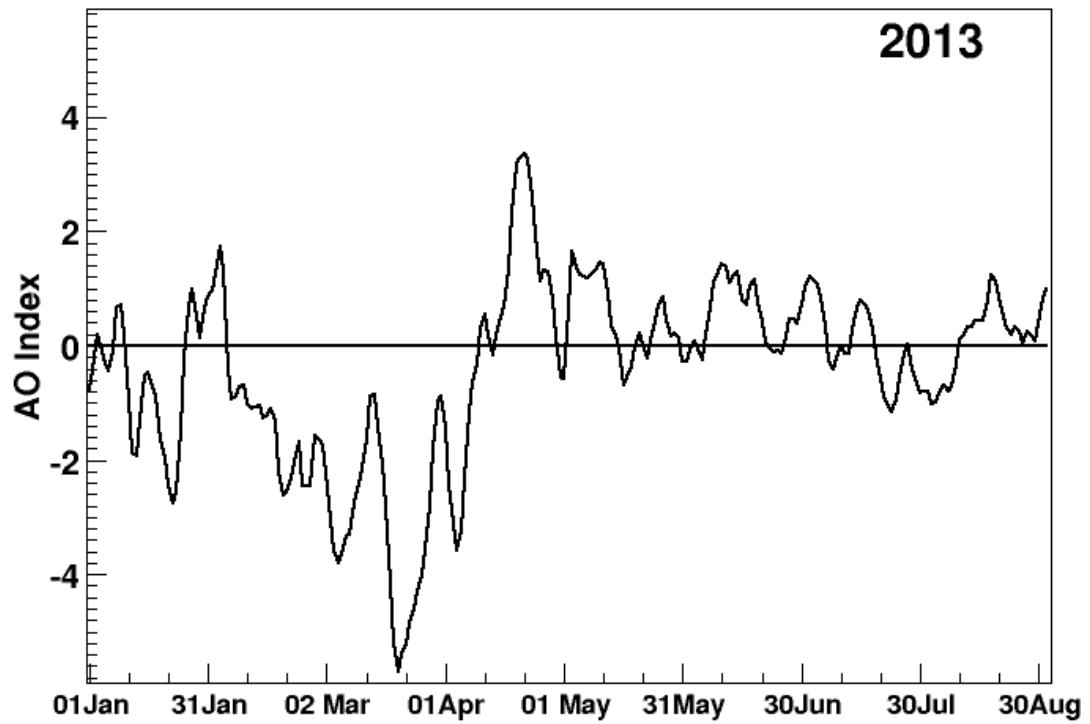


Figure 14: Evolution of AO Index during 2013